

Autonomous and Continuous As-is 3D Thermal Mapping for Construction Environments

John Ramel Y. Abanes^{1,*}, Samuel A. Prieto^{2,*}, and Borja García de Soto^{3,*}

Abstract—Thermal Point Clouds (TPCs) can provide valuable information during the inspection and assessment of the performance of buildings and for energy auditing; however, it faces two issues regarding data: scanning time and redundancy optimization. The use of continuous and discrete scanning paths can decrease collection times, and the automation of the process can optimize data redundancy and accuracy. However, the current state of the art lacks systems that perform autonomously over a continuous path. This study presents a platform for the continuous and automated generation of TPCs that improves real-time scan quality evaluations and path optimization.

I. INTRODUCTION

The 2022 Energy Efficiency report by the International Energy Agency (IEA) [1] indicates that differences between efficient and inefficient thermal planning for residential structures can triple heating costs. Therefore, thermal analysis of structures is an increasingly important field in construction to promote sustainability. Advancements in computer vision have allowed for more efficient methods in creating Thermal Building Information Models (TBIM) to improve energy auditing of buildings [2]. TBIM generation has also improved through the automation of data collection. Common practices involve thermal mapping via infrared cameras along with LiDAR. This can be combined with algorithms such as Simultaneous Localization and Mapping (SLAM) and Structure from Motion (SfM) to create a thermal model of a building.

However, temporal and spatial non-uniformity issues can arise when creating TBIMs [3]. For example, temperature readings can vary over time due to environmental changes or to the change in the camera's internal temperature—necessitating calibration. Temperature readings can also vary spatially, as seen in the discrepancies in readings from different angles of view [4], [5]. As summarized in the Literature Review section, the spatial and temporal non-uniformity issues dominate TBIM generation approaches—especially in three-dimensional models. Generally, TBIM generation models can be categorized based on data collection path and type. The path involves a selected number of discrete points or a continuous data stream. The collection type can either be manual or automatic. The resulting combinations of path and type are used to classify existing work since they all tackle the issues of non-uniformity similarly. A survey of existing

literature shows a need for more development in continuous and automated models.

This study uses the Robotnik SUMMIT XL platform to present a prototypical automated and continuous TBIM generation system. The continuous path allows for faster scans, reducing the impact of temporal variations in the environment. Meanwhile, the automation of the system presents the stage for algorithms that can minimize dark spots and increase data redundancy in real time.

The reaming of this paper is organized as follows: Section II discusses the state-of-the-art and currently employed methods in TBIM generation. Section III discusses the theory and flow diagrams for the proposed system. Section IV documents the experimentation process and any additional steps taken during testing. Section V summarizes the results, and Sections VI gives concluding remarks and thoughts on future research.

II. LITERATURE REVIEW

A. Thermal Mapping

Thermal mapping is the projection of temperature onto spatial information. Depending on the target structure, the mapping may be two-dimensional (2D), 2D with depth (2.5D), or three-dimensional (3D). 2D maps typically overlay information from a thermal camera with an RGB camera and are most commonly used in analyzing flat surfaces and façades. For example, [6] demonstrates the use of classification algorithms for structural crack detection. Next, 2.5D maps apply depth to a 2D map to distinguish the structure's geometry. [7] shows how thermal information can be mapped with depth using LiDAR. Alternatively, [8] demonstrates a low-cost solution that implements Structure from Motion (SfM) algorithms to extrapolate a 2.5D map from stereo cameras. 3D maps incorporate the fusion of multiple 2.5D projections. Although LiDAR can have up to 360° field of view, the same cannot be said for thermal cameras. 3D maps are thus created by stitching together multiple 2.5D scans. This stitching process warrants an increased amount of precision. As a result, many applications rely heavily on LiDAR SLAM. While visual SLAM provides a better potential for pattern recognition [9], LiDAR SLAM's capacity for real-time 360° localization is more valuable in creating TPCs.

*S.M.A.R.T. Construction Research Group, Division of Engineering, New York University Abu Dhabi (NYUAD), Experimental Research Building, Saadiyat Island, P.O. Box 129188, Abu Dhabi, United Arab Emirates

¹Undergraduate Student, john.abanes@nyu.edu

²Post-Doctoral Associate, samuel.prieto@nyu.edu

³Assistant Professor, garcia.de.soto@nyu.edu

TABLE I
SUMMARY OF PAPERS USED IN THE LITERATURE REVIEW

Ref ID	First Author	Date	Sensors Used*	Data Collection Method	Target	Environment	Dimension	Data Collection Path
[7]	Wang	2013	L, I	Manual	Façade	Exterior	2.5D	Discrete
[8]	Vidas	2013	I, C	Manual	Building	Interior	2.5D	Discrete
[10]	Zhu	2021	L, I	Manual	Façade	Exterior	3D	Discrete
[11]	Yun	2022	L, I, C	Manual	Façade	Exterior	3D	Continuous
[12]	Schischmanow	2022	L, I, C	Manual	Building	Both	3D	Continuous
[6]	Van Nguyen	2018	I, C	Automated	Façade	Exterior	2D	Discrete
[13]	Adán	2019	L, I, C	Automated	Building	Interior	3D	Discrete
[14]	Kim	2017	L, I, C	Automated	Building	Interior	3D	Discrete
[15]	Kumar	2017	I, C	Automated	Building	Interior	2D	Continuous, but Non-mapping

*(L) LiDAR, (I) infrared camera, (C) RGB camera

As seen in Table I, LiDAR is prevalent in creating 3D TBIMs. However, thermal cameras tend to be more out of focus and/or have lower resolution than RGB cameras. As a result, algorithms that prioritize edge detection [10] and object recognition [14] additionally use RGB cameras.

B. Data Collection Type and Path

Table I lists various researched implementations of TPC creation. Keywords for searching include "thermal point clouds", "Building Information Model (BIM)", "thermal and point cloud data fusion", and "thermal mapping/modeling". The term "automated" was added to specifically identify autonomous TBIM generation techniques. The basis for an autonomous system is the ability to perform evaluations and path modifications in real time. For example, [16] presents a system that involves an automated robot that can perform 3D mapping continuously. However, the data processing occurs offline (e.g., after all the data collection) and therefore lacks the capability for recursive self-evaluation. As a result, this paper was not included in the review.

TPCs can be generated in manual or automated manners. Manual methods collect data in a pre-established manner, whereas automated procedures can update the path depending on spontaneous parameters such as scan quality or completeness. In [11], the sensors are attached to a manually driven car, whereas in [12], the sensors are handheld. Since the TPC is only generated after all the data collection, this implies that manual systems are unable to effectively model regions outside the sensors' field of vision. Furthermore, in the case of a thermal camera attached atop a car, the readings for points on the roadside will always be at an angle with respect to the normal plane. This creates further errors in the readings, as discussed in [4] and [5]. In contrast, automated systems such as in [13] can perform real-time evaluations of the scan, recursively determining which areas require more data collection. This optimization of data redundancy allows for more accurate readings and fewer dead zones. However, their system performs stop-and-go data collection instead of continuous scanning, which results in less efficiency.

The data collection path is also important when tackling the scanning time. In [11] and [12], the continuous path allows for faster scan times compared to discrete methods. However, the manual data collection leads to issues previously discussed. In [15], the system drives autonomously

and continuously but does not perform thermal mapping. In the current literature, there is a lack of systems that autonomously create thermal maps in a continuous manner.

III. METHODOLOGY

This section presents a system that implements an autonomous and continuous method to generate TPCs. The SUMMIT-XL Robot is used as a platform. A FLIR A65 Infrared Camera ($90^\circ \times 69^\circ$ FOV and a resolution of 640×512) and an Ouster OS1 LiDAR ($360^\circ \times 45^\circ$ FOV and a resolution of 60×1024) are mounted on the robot to collect thermal and 3D information (Fig. 1 and Fig. 2). Furthermore, the thermal camera is mounted on a FLIR Pan-Tilt unit (PTU-E46-17) for two extra controllable degrees of freedom (range of motion of $\pm 159^\circ$ in pan and -47° to $+31^\circ$ in tilt, and a resolution of 0.129°). This is a novel implementation in the field of TBIMs, as most systems just relate the camera and the robot body via a fixed frame. The system has been tested in a cluttered lab space of 80 m^2 , an environment similar to what the system might encounter in a real implementation.



Fig. 1. General view of hardware setup and robotic platform



Fig. 2. Close up of LiDAR, thermal camera and PTU

A. Calibration between thermal camera and LiDAR

To properly connect the 2D thermal information (X_t, Y_t) with the 3D geometric information (X_p, Y_p, Z_p) , an extrinsic calibration needs to be performed between the FLIR thermal camera and the Ouster LiDAR. To obtain this geometric correspondence, the method proposed by Adan et al. [13] was used. A set of small landmarks consisting of ice cubes with a reflective surface (Fig. 3) was used to obtain common points easily visible in the thermal image (due to the low temperature) (Fig. 4) and the reflectance image from the LiDAR (due to the highly reflective surface) (Fig. 5).



Fig. 3. Ice cubes with reflective surface used as calibration landmarks

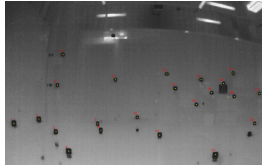


Fig. 4. Thermal picture with locations (numbers in red) of landmarks



Fig. 5. Reflectance picture with locations (numbers in red) of landmarks

The computed transformation matrix M_e between individual points is presented in (1).

$$\begin{pmatrix} \lambda X_f \\ \lambda Y_f \\ \lambda \end{pmatrix} = \begin{pmatrix} r_{11} & r_{12} & r_{13} & r_{14} \\ r_{21} & r_{22} & r_{23} & r_{24} \\ r_{31} & r_{32} & r_{33} & r_{34} \end{pmatrix} \begin{pmatrix} X_p \\ Y_p \\ Z_p \\ 1 \end{pmatrix} \quad (1)$$

The matrix M_e and its r_{ij} components can be calculated by applying the Moore-Penrose pseudoinverse, knowing the coordinates of each one of the landmarks both in the thermal and the reflectance images. After performing the calibration and computing the transformation matrix, the Mean Squared Error (MSE) of the distance between the actual position of the landmarks' centroids and their projected position was 3.33 pixels. Given that the resolution of the thermal camera is 640x512 pixels, the error is negligible for the short and medium distances of the space investigated in this study.

Additionally, an extra transformation needs to be performed considering the angles from the PTU (M_p) and the robot's real-time position calculated by the 3D SLAM (M_r). The final transformation matrix M_t is calculated by combining the three transformations $M_t = M_e \cdot M_p \cdot M_r$.

B. TPC generation

The process used for creating the thermal point cloud is outlined by the flowchart shown in Fig. 6.

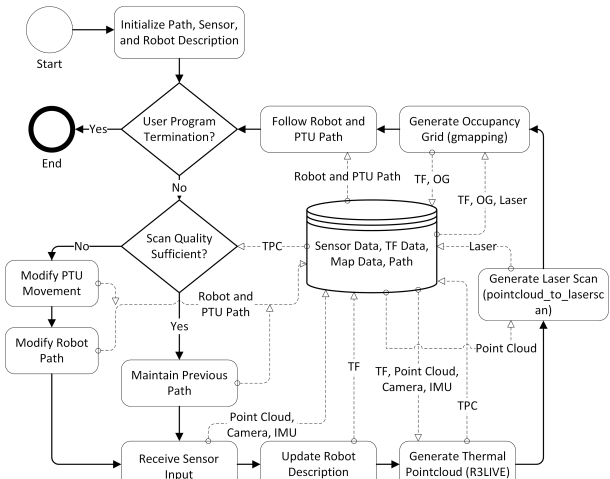


Fig. 6. Main steps and processes of the proposed Thermal Mapping. Acronyms used: Occupancy Grid (OG), Pan-Tilt Unit (PTU), Inertial Measurement Unit (IMU), and Transformations (TF)

Upon starting, the algorithm initializes the scanning path, sensors, and the robot description—which publishes the transformation frames (TF) relating the robot, sensors, and PTU. The algorithm will proceed until the end user sends a termination request. With each iteration of the loop, the algorithm evaluates the TPC and modifies the robot and PTU path. After receiving the sensor input and updating the robot description, the algorithm generates two datasets: a 3D TPC and a 2D occupancy grid (OG) used for navigation. The 3D TPC is created by applying the R3LIVE algorithm [17] with the point cloud, thermal image, IMU information, and all the transformations involved in stitching the thermal information to the point cloud as the robot moves. The 2D OG is created by first converting the point cloud to a 2D laser scan ROS topic and then applying the gmapping algorithm [18]. These maps are updated continuously with each loop cycle, resulting in an automated and continuous TPC generation algorithm. All the source code is available on Github [19].

IV. RESULTS AND DISCUSSION

This section discusses the implementation of the thermal mapping algorithm discussed in Section III-B (TPC generation). Different views of the space where the experiment was conducted are shown in Fig. 7 and Fig. 8.



Fig. 7. General view (A) where the experiment was conducted



Fig. 8. General view (B) where the experiment was conducted

The process (Fig. 6) includes a sub-task that evaluates the scan quality and completeness (e.g., dark zones) and updates the robot and PTU path. However, this is still a work in progress; therefore, no iterative modifications to the path are done in the current version. Using the OG created by the SLAM algorithm [18], a costmap is used to autonomously path find towards the preset destination (Fig. 9). Simultaneously, the R3LIVE algorithm [17] is used to continuously generate a TPC (Fig. 10).

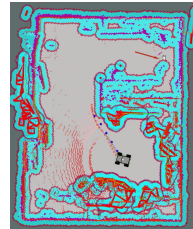


Fig. 9. Navigation Costmap

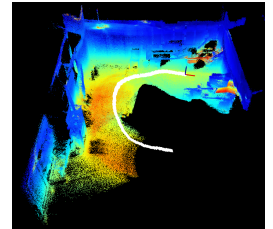


Fig. 10. Real-time Generated TPC

It took the robot to autonomously reconstruct the TPC in this study about 1'30". If the same process was done by a static approach (stop-and-go scanning), at least 3 different scan locations would be needed to deal with all the occlusions for the same space, with a scanning time of about 2'45" per location. A handheld approach would be

close in time to the one of the robot, but other factors, such as stability, would need to be addressed.

The accuracy of the thermal data was not considered because the changes in temperature in the TPC were evaluated at a qualitative level. Some conditions observed, such as thermal bridges or lack of insulation, can be clearly identified and do not need precise temperature information.

V. CONCLUSIONS, LIMITATIONS, AND OUTLOOK

The generation of TPCs, necessary for creating 3D TBIMs, faces the issue of temporal and spatial problems. Slow scan times can lead to deviations caused by environmental variations, such as the time of day. Thermal imaging also has errors when measured at an angle to the scan surface's normal. Continuous scan paths can resolve temporal issues, and automated systems can perform real-time scan analysis to assess data quality. However, the current literature lacks systems that are both continuous and automated. This paper presents a prototype of such a system, which can directly be augmented with improvements based on the use case.

The proposed implementation presents a potential archetype for the autonomous and continuous generation of as-is 3D thermal mapping (i.e., generation of TPCs) in construction environments. Further improvements can be added to increase efficiency. For example, the OG and the thermal map can be reconciled through Kalman filters to increase navigational and data accuracy. Continued developments to the PTU and scan completeness algorithms can also increase efficiency. Further real experimentation of all the steps involved in the methodology will be tackled in future work, as well as using this approach to develop digital twins to assess the thermal performance of buildings.

ACKNOWLEDGEMENT

Thanks to Mr. Giakoumidis (NYUAD Kinesis CTP Lab) for assisting with the power systems and automation of the robotic platform and Mr. Montalvo Navarrete (NYUAD Advanced Manufacturing Workshop) for his support in the 3D-printed mount for the thermal camera. This work has benefited from the collaboration with the NYUAD Center for Interacting Urban Networks (CITIES), funded by Tamkeen under the NYUAD Research Institute Award CG001.

REFERENCES

- [1] IEA, "Energy efficiency 2022," IEA, Paris, 2022. [Online]. Available: <https://www.iea.org/reports/energy-efficiency-2022> (visited on 02/14/2023).
- [2] Y. K. Cho, Y. Ham, and M. Golpavar-Fard, "3d as-is building energy modeling and diagnostics: A review of the state-of-the-art," *Advanced Engineering Informatics*, Infrastructure Computer Vision, vol. 29, no. 2, pp. 184–195, Apr. 1, 2015, ISSN: 1474-0346. DOI: 10.1016/j.aei.2015.03.004.
- [3] A. Ramón, A. Adán, and F. Javier Castilla, "Thermal point clouds of buildings: A review," *Energy and Buildings*, vol. 274, p. 112425, Nov. 1, 2022, ISSN: 0378-7788. DOI: 10.1016/j.enbuild.2022.112425.
- [4] X. Zhao, X. Jia, Q. Shi, J. Wu, and P. Li, "Effect of angle of view on temperature measurement error by multiple regression method," *Journal of Physics: Conference Series*, vol. 2026, no. 1, p. 012041, Sep. 2021, Publisher: IOP Publishing, ISSN: 1742-6596. DOI: 10.1088/1742-6596/2026/1/012041.
- [5] M. Litwa, "Influence of angle of view on temperature measurements using thermovision camera," *IEEE Sensors Journal*, vol. 10, no. 10, pp. 1552–1554, Oct. 2010, Conference Name: IEEE Sensors Journal, ISSN: 1558-1748. DOI: 10.1109/JSEN.2010.2045651.
- [6] L. Van Nguyen, S. Gibb, H. X. Pham, and H. M. La, "A mobile robot for automated civil infrastructure inspection and evaluation," in *2018 IEEE International Symposium on Safety, Security, and Rescue Robotics (SSRR)*, ISSN: 2475-8426, Aug. 2018, pp. 1–6. DOI: 10.1109/SSRR.2018.8468642.
- [7] C. Wang, Y. K. Cho, and M. Gai, "As-is 3d thermal modeling for existing building envelopes using a hybrid LIDAR system," *Journal of Computing in Civil Engineering*, vol. 27, no. 6, pp. 645–656, Nov. 1, 2013, Publisher: American Society of Civil Engineers, ISSN: 1943-5487. DOI: 10.1061/(ASCE)CP.1943-5487.0000273.
- [8] S. Vidas, P. Moghadam, and M. Bosse, "3d thermal mapping of building interiors using an RGB-d and thermal camera," in *2013 IEEE International Conference on Robotics and Automation*, ISSN: 1050-4729, May 2013, pp. 2311–2318. DOI: 10.1109/ICRA.2013.6630890.
- [9] J. Cheng, L. Zhang, Q. Chen, X. Hu, and J. Cai, "A review of visual SLAM methods for autonomous driving vehicles," *Engineering Applications of Artificial Intelligence*, vol. 114, p. 104992, Sep. 1, 2022, ISSN: 0952-1976. DOI: 10.1016/j.engappai.2022.104992.
- [10] J. Zhu, Y. Xu, Z. Ye, L. Hoegner, and U. Stilla, "Fusion of urban 3d point clouds with thermal attributes using MLS data and TIR image sequences," *Infrared Physics & Technology*, vol. 113, p. 103622, Mar. 1, 2021, ISSN: 1350-4495. DOI: 10.1016/j.infrared.2020.103622.
- [11] S. Yun, M. Jung, J. Kim, et al., "STheReO: Stereo thermal dataset for research in odometry and mapping," in *2022 IEEE/RSJ International Conference on Intelligent Robots and Systems (IROS)*, ISSN: 2153-0866, Oct. 2022, pp. 3857–3864. DOI: 10.1109/IROS47612.2022.9981857.
- [12] A. Schischmanow, D. Dahlke, D. Baumbach, I. Ernst, and M. Linkiewicz, "Seamless navigation, 3d reconstruction, thermographic and semantic mapping for building inspection," *Sensors*, vol. 22, no. 13, p. 4745, Jan. 2022, Number: 13 Publisher: Multidisciplinary Digital Publishing Institute, ISSN: 1424-8220. DOI: 10.3390/s22134745.
- [13] A. Adán, S. A. Prieto, B. Quintana, T. Prado, and J. García, "An autonomous thermal scanning system with which to obtain 3d thermal models of buildings," in *Advances in Informatics and Computing in Civil and Construction Engineering*, I. Mutis and T. Hartmann, Eds., Cham: Springer International Publishing, 2019, pp. 489–496, ISBN: 978-3-030-00220-6. DOI: 10.1007/978-3-030-00220-6_58.
- [14] P. Kim, J. Chen, and Y. K. Cho, "Robotic sensing and object recognition from thermal-mapped point clouds," *International Journal of Intelligent Robotics and Applications*, vol. 1, no. 3, pp. 243–254, Sep. 1, 2017, ISSN: 2366-598X. DOI: 10.1007/s41315-017-0023-9.
- [15] Y. Kumar, J. Rahul, R. Harikrishnan, A. M. T. P, and P. Sreedharan, "Design and analysis of building diagnostics robot," *Journal of Physics: Conference Series*, vol. 2070, no. 1, p. 012242, Nov. 2021, Publisher: IOP Publishing, ISSN: 1742-6596. DOI: 10.1088/1742-6596/2070/1/012242.
- [16] D. De Pazzi, M. Pertile, and S. Chioldini, "3d radiometric mapping by means of LiDAR SLAM and thermal camera data fusion," *Sensors*, vol. 22, no. 21, p. 8512, Jan. 2022, Number: 21 Publisher: Multidisciplinary Digital Publishing Institute, ISSN: 1424-8220. DOI: 10.3390/s22218512.
- [17] J. Lin and F. Zhang, "R3live: A robust, real-time, RGB-colored, LiDAR-inertial-visual tightly-coupled state estimation and mapping package," in *2022 International Conference on Robotics and Automation (ICRA)*, May 2022, pp. 10672–10678. DOI: 10.1109/ICRA46639.2022.9811935.
- [18] G. Grisetti, C. Stachniss, and W. Burgard, "Improved techniques for grid mapping with rao-blackwellized particle filters," *IEEE Transactions on Robotics*, vol. 23, no. 1, pp. 34–46, Feb. 2007, Conference Name: IEEE Transactions on Robotics, ISSN: 1941-0468. DOI: 10.1109/TRO.2006.889486.
- [19] J. R. Abanes, S. A. Prieto, and B. García de Soto, "SMART-NYUAD/TPCMapping," Github. (2023), [Online]. Available: <https://github.com/SMART-NYUAD/TPCMapping/tree/master> (visited on 04/28/2023).